Journal of Electronic Science and Technology xxx (xxxx) xxx

Contents lists available at ScienceDirect

Journal of Electronic Science and Technology

journal homepage: www.keaipublishing.com/en/journals/journal-of-electronic-science-and-technology/

Dual-mode terahertz extended interaction oscillator driven by a pseudospark-sourced sheet electron beam☆

Jie Xie [a,*], Xue-Song Yuan [a], Liang Zhang [b], Adrian W. Cross [b], Hua-Bi Yin [b], Qing-Yun Chen [a], Tong-Bin Yang [a], Xiao-Tao Xu [a], Yang Yan [a], Lin Meng [a]

[a] School of Electronic Science and Engineering, University of Electronic Science and Technology of China, Chengdu, 610054, China
[b] Department of Physics, University of Strathclyde, Glasgow, G4 0NG, UK

ARTICLE INFO

Keywords:
Dual-mode operation
Extended interaction oscillator (EIO)
High-power radiation
Pseudospark-sourced electron beam
Sheet electron beam (SEB)
Terahertz

ABSTRACT

A terahertz dual-mode extended interaction oscillator (EIO) driven by a pseudospark-sourced sheet electron beam (SEB) was presented. The major advantages of the newly developed circuit include 1) high-density SEB interacting with the TM_{11} and TM_{31} modes, respectively, and 2) high output power of over 1 kW at the sub-terahertz frequency range. Two different types of 2π modes and their output characteristics were studied, and the circuit was optimized to ensure efficient outputs of two standing-wave modes. The three-dimensional (3D) particle-in-cell (PIC) simulation predicts the maximum output power of 1.3 kW with a 3-dB bandwidth of ~0.5 GHz at 303 GHz when operating at the TM_{11} mode, and 3.18 kW, 3-dB bandwidth of ~0.85 GHz at 364 GHz when operating at the TM_{31} mode.

1. Introduction

In the recent decades, high-power radiation sources at the millimeter waves and terahertz (THz) radiation frequency bands from 100 GHz to 1 THz have gained significant interest due to their numerous exciting applications, such as broadband wireless and high data rate communications, high resolution radar and imaging, and biomedical and plasma diagnostics [1–6]. Driven by these applications, the THz radiation sources with high output power had made great progress. Among various THz radiation sources, vacuum electronic devices (VEDs) are intrinsically superior with handling high power or high power density due to the electrons moving in vacuum without scattering [2,7,8]. The sheet electron beam extended interaction oscillator (SEBEIO), as an important kind of VEDs achieving high output power and maintaining a compact structure, has gained considerable attention as a promising THz oscillation source due to its feasibility, stability, and high gain per unit length [2,9]. In the THz frequency band, one of the major factors limiting the development of THz devices is the maximum electron beam current density at the interaction region. In our design, a pseudospark-sourced (PS) electron beam was used to drive SEBEIO because of its high current density (10^8 A/m^2), high brightness (10^{12} A/(m^{2}rad^2)), low vacuum requirements, and its propagation with no need for any external focusing magnetic fields [10–14].

A number of SEBEIO experiments have been reported. For example, a W-band extended interaction klystron (EIK) was reported by Pasour et al., which produced 7.5-kW output power. It was driven by a 20-kV, 4-A sheet beam and the efficiency was ~17% [15]. At

☆ Publishing editor: Yu-Lian He.

* Corresponding author.
E-mail addresses: xiejie@std.uestc.edu.cn (J. Xie), yuanxs@uestc.edu.cn (X.-S. Yuan), liang.zhang@strath.ac.uk (L. Zhang), a.w.cross@strath.ac.uk (A.W. Cross), h.yin@strath.ac.uk (H.-B. Yin), cqy@std.uestc.edu.cn (Q.-Y. Chen), yangtongbin@std.uestc.edu.cn (T.-B. Yang), xxt@std.uestc.edu.cn (X.-T. Xu), yanyang@uestc.edu.cn (Y. Yan), meng@uestc.edu.cn (L. Meng).

https://doi.org/10.1016/j.jnlest.2021.100093
Received 13 September 2020; Received in revised form 11 November 2020; Accepted 25 February 2021
Available online xxxx

University of California, Davis, a W-band sheet beam klystron with 10-kW output power, 20-ms pulse duration, and 17-dB gain was presented [16]. An extended interaction oscillator (EIO) with ~10-W continuous-wave (CW) output power operated at 220 GHz–270 GHz and an EIK with 25-W pulsed power operated at 250 GHz–276 GHz have been designed by Communication & Power Industries [17]. The high-power W-band SEBEIO with 6-kW maximum output power driven by the 47.2-kV and 2.1-A sheet electron beam (SEB), and more than 1.2-kW average power has been designed and tested by Wang et al. at University of Electronic Science and Technology of China [18]. The researchers at University of Strathclyde presented the SEBEIO output power of over 10 W at a frequency of ~0.2 THz and the W-band SEBEIO with the peak output power up to 1.2 kW [19,20]. As discussed in all of the above EIOs and EIKs, they have achieved excellent performance in a single frequency band. However, to develop SEBEIO using the same circuit to work in dual frequency bands is significantly beneficial for reducing the size, cost, and weight of THz sources. This paper introduces the design of dual-mode SEBEIO, which works at both 0.30 THz and 0.36 THz with the tuning bandwidth of 0.50 GHz and 0.85 GHz, respectively, and peak power of more than 1.3 kW.

2. Pseudospark-sourced sheet electron beam (PS-SEB)

In the recent decades, the PS-generated high-density and energetic-pulsed electron beam has attracted significant interest due to its potential and growing applications in the areas of high-power radiation generation, extreme ultraviolet (EUV) sources, intense X-rays, free electron masers, and so on [11–14,19–28]. The PS discharge is a self-sustained, transient, and axially symmetric discharge at the low-pressure (50 mTorr–500 mTorr) gas conditions. It has the ability to produce the electron beams combined the highest current density and brightness with low emittance of 15 mm mrad, fast current rise up to 10^{12} A/s, and high power density of ~10^{19} W/cm^2, which is catered to the requirement for high-power sources of millimeter waves and THz radiation, as well as accelerators, such as backward wave oscillators (BWOs), EIOs, and free-electron lasers (FELs) [29–31]. In recent years, the PS electron beam achieved further progress and various pencil PS discharge electron beams have been investigated by the particle-in-cell (PIC) simulations and experiments [32–36].

Nevertheless, one of the major factors limiting high-power vacuum microwave radiation sources to higher frequencies is the need of transporting beams with higher current density, due to the decrease of high-frequency circuit transverse dimensions with the wavelength. As the frequency of VEDs increasing to 100 GHz or beyond that, the beam diameter has to be approximately one-tenth of the wavelength or less in pencil-beam VEDs. While, the use of SEB can overcome this difficult owing to its larger cross-sectional dimensions. Compared with the pencil beam, the advantage of SEB is that the space charge effect is small and a higher current can be achieved by increasing the width of beam, which helps to increase the output power. It is a challenge for the thermionic cathode to generate a sufficiently high-perveance and uniform beam, since it needs a complicate focusing system to confine SEB. However, it is much simpler in a PS discharge system since a plasma channel formed in the system can confine SEB and has no need for an external magnetic field. In the experiment, a post-acceleration modulator with a cross-sectional size of 1.00 mm × 0.17 mm of SEB was used, and PS-SEB with a peak current of 21.5 A was measured without an external focusing magnetic field [20]. PS-SEB with the current density of ~1 kA/cm2 has been generated using a sheet beam plasma cathode electron gun [37]. The influence of geometrical design parameters on the high current density PS-SEB has been analyzed by the PIC simulation models and experiments [38,39]. In this article, SEB generated by PS is used to drive the dual-mode SBEIO structure. In our design of the PS discharge system, it has a four-gap PS discharge setup which consists of a hollow cathode (HC) with a central hole and an anode with an aperture to extract the electron beam, as shown in Fig. 1. The anode and HC are separated by the dielectric insulators. The PS discharge occurs under suitable low pressure (typically 50 mTorr–500 mTorr) in the system, as HC is applied with a negative high voltage and the anode is grounded. In the process of the PS discharge, an electron beam with a very large current can be generated. When the high current density and brightness beam propagates through the anode and the interaction circuit, the front edge of the beam ionizes the background gas and generates a plasma channel. Subsequently, beam electrons expel some of the plasma electrons, while the heavier ions remain fixed. Therefore, a positive ion channel is formed to focus the PS electron beam. PS-SEB can be extracted using a collimator with a rectangular aperture placed at the end of the anode. The rectangular aperture of the collimator should be located at the same axial center as the cylindrical aperture of the anode.

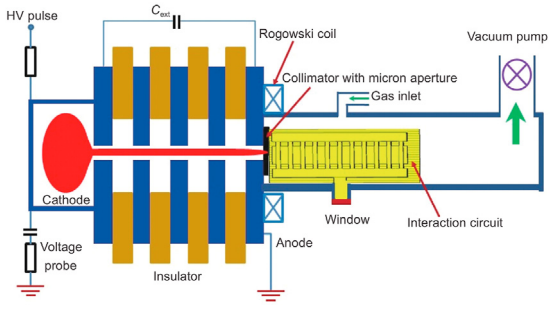

Fig. 1. SBEIO composed of a four-gap PS discharge system and the interaction circuit.

3. Design of the SEBEIO circuit

The SEBEIO circuit composes of eleven gaps and two symmetrical coupling cavities on both sides of the structure, as shown in Fig. 2. A 0.90 mm × 0.19 mm rectangular beam tunnel passes through the center of the slots and intersects with the slow-wave structure. It combines the advantages of traveling-wave tubes and klystrons and has the capacity of handling high output power in the millimeter-wave and THz-frequency regimes. EIO, typically, works at the fundamental mode (TM_{11} mode), since it is the easiest mode to achieve the start-oscillation condition [20,30,40]. While in recent years, EIO working at the high-order mode has become more and more attractive due to its higher beam power and larger power capacity [41–43].

3.1. Mode analysis

The three-dimensional (3D) SEBEIO model is shown in Fig. 2. The ladder cavity is a periodic standing-wave circuit along the longitudinal direction. Based on the distribution pattern of the axial electric field in the cavity along the transverse direction, the resonant modes of the ladder cavity are usually named as TM_{n1} and the index n is determined by the variation in the distribution pattern of the axial electric field along the transverse direction. The axial electric field distributions of the fundamental mode TM_{11} and the high-order mode TM_{31} at the cross-section are shown in Fig. 3. The E_z fields in the TM_{11} and TM_{31} modes are unidirectional and concentrating at the beam area so that the interaction with the electron beam is effective. The beam-mode coupling is determined by the characteristic impedance R/Q, expressed as $R/Q = (\int_a^b E_z \mathrm{d}l)^2/2\omega W$, where R is the equivalent resistance of cavity, Q is the quality factor, ω is the resonant angular frequency, and W is the stored energy in the cavity, which is a measure of E_z fields interacting on the electrons. The TM_{31} mode provides a stronger electric field concentrating at the tunnel area as well as high R/Q, as shown in Fig. 3. Table 1 lists the frequencies, inherent quality factors Q_0, and characteristic impedances R/Q of the cavity with different modes. R/Q indicates the strength of the interaction between the electron beam and the high-frequency field in the cavity. A cavity with higher R/Q has the potential to achieve higher output power. The electric field of the 2π mode is in the same direction in each gap as shown in Fig. 4, which contributes to a higher R/Q value. The 2π mode also provides the electric field with the same direction in each gap for sufficient beam-wave interactions, as shown in Fig. 5. The TM_{31}-2π mode has the highest R/Q, which is beneficial for SEBEIOs when operating at a high-order mode. Meanwhile, the 2π mode corresponds to the largest fundamental spatial harmonic and consequently has the largest structure dimension along the axial direction [44,45].

3.2. Dispersion characteristic

The key issue for EIO operating in a dual-mode condition is the mode competition. An effective method is to make the frequency interval between the operating modes wide enough. Due to the limited periodic structure of the multigap resonant cavity, the dispersion curve consists of a series of discrete frequency points. The dispersion curve of the designed radio frequency (RF) circuit computed by the CST Microwave Studio is shown in Fig. 6. It is an effective approach to identify the possible mode competition and self-oscillation. The red curve with dot markers represents the TM_{11} mode, and the blue curve with triangular markers represents the TM_{31} mode. The operating voltages of the TM_{11}-2π and TM_{31}-2π modes are 18.5 kV–22.5 kV and 27.5 kV–34 kV, respectively, and the synchronous beam voltages are 20 kV and 30 kV, respectively, as shown in Fig. 6. The operating voltage of the TM_{11}-2π mode is smaller than that of the TM_{31}-2π mode. As shown in Fig. 6, the 22.5-kV beam line is far away from the TM_{31}-2π mode point so the competition between these two 2π modes can be suppressed. However, the 30-kV beamline intersects with the TM_{11}-17/10π mode, which indicates the mode competition between these two modes may occur as the oscillation startup condition is satisfied.

The normalized E_z-field distribution of the TM_{31}-2π mode along the beam tunnel is significantly stronger than that of the TM_{11}-17/10π mode, as shown in Fig. 7 (a). Through estimation using the axial electric field, the characteristic impedance R/Q of the TM_{31}-2π mode is about 10 times than that of the TM_{11}-17/10π mode, as shown in Table 1. The normalized E_z-field distributions of the TM_{31}-2π

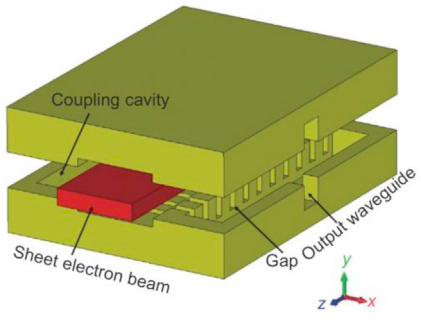

Fig. 2. Schematic drawing of the SEBEIO circuit with eleven gaps.

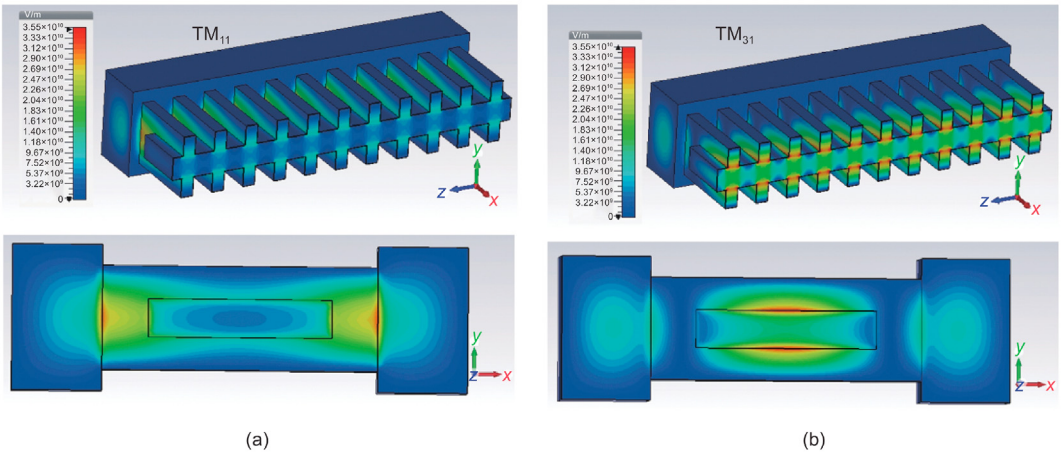

Fig. 3. Electric field magnitude for (a) TM_{11} mode and (b) TM_{31} mode at the cross-section.

Table 1
Basic parameters of the eigenmodes.

Mode	Frequency (GHz)	R/Q (Ω)	Q_0
TM_{11}-2π	304.1	91	675
TM_{11}-19/10π	304.9	74	671
TM_{11}-17/10π	312.1	85	712
TM_{31}-2π	366.7	865	837
TM_{31}-19/10π	367.6	702	825

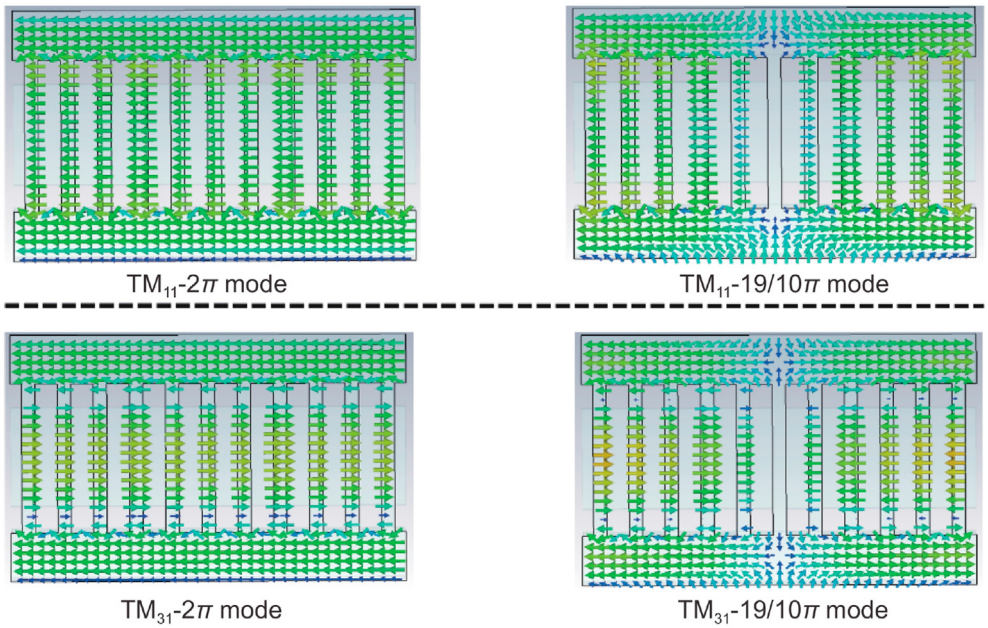

Fig. 4. E_z-field distributions of TM_{11}-2π, TM_{11}-19/10π, TM_{31}-2π, and TM_{31}-19/10π modes along the z-axis.

and TM_{11}-17/10π modes along the cross-section are illustrated in Fig. 7 (b). In the beam tunnel area, the E_z field strength of the TM_{31}-2π mode is stronger than that of the TM_{11}-17/10π mode. Reflected from the results of the R/Q values and field distributions of these two modes, the competition between the TM_{11}-17/10π mode and the TM_{31}-2π mode is hard to be excited.

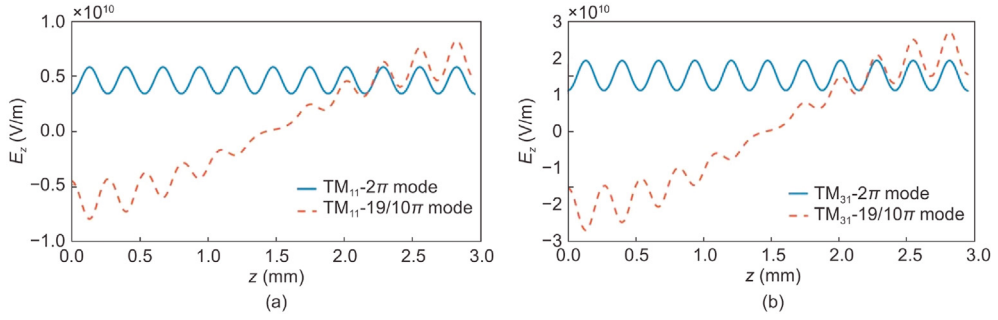

Fig. 5. Normalized E_z distributions along the z-axis of (a) TM_{11}-2π and TM_{11}-19/10π modes and (b) TM_{31}-2π and TM_{31}-19/10π modes.

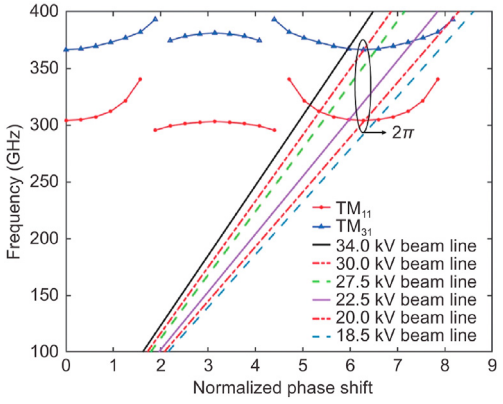

Fig. 6. Dispersion curve of the SEBEIO circuit.

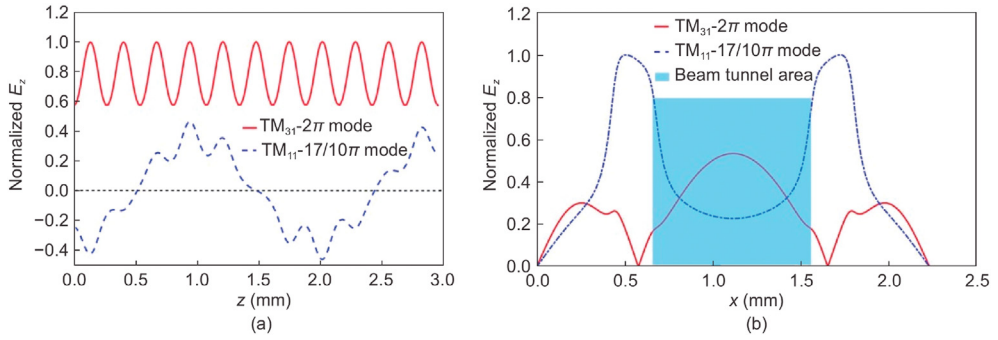

Fig. 7. E_z-field distributions of the TM_{31}-2π and TM_{11}-17/10π modes (a) along the beam tunnel direction and (b) along the cross-section of cavity.

4. PIC simulation

To validate our design, the 3D PIC simulation was used to demonstrate the performance of the dual-mode SEBEIO. As the operating frequency of VEDs increasing up to the THz range, the Ohmic loss caused by the metal material has a significant impact on the performance. The copper conductivity at the THz frequency range is much smaller than that in the direct current (DC) case. The nonideal surface losses at the THz frequency caused by surface roughness have been reported in Ref. [46]. In our simulation, the conductivity σ of the background material was set as 1.1×10^7 S/m ($<\sigma_{Cu}/5$, $\sigma_{Cu} = 5.8 \times 10^7$ S/m for copper), taking into consideration the Ohmic loss. A beam current of 3 A with the voltages of 24 kV and 37 kV is respectively injected into the interaction circuit. A stable output signal with 51.8 V/79.4 V (equivalent to output power of 1.34 kW/3.15 kW) is obtained at 303.4 GHz/364.5 GHz, respectively, as depicted in Fig. 8. The E_z-field distributions along the z-axis demonstrate SEBEIO can operate at the TM_{11}-2π and TM_{31}-2π modes without mode competition, which agrees well with the above theoretical analysis of the circuit's dispersion curve. Fig. 9 shows the output power, frequency, and the starting oscillation time versus the voltage. It predicts that the output power changes from 0.94 kW to 1.34 kW in the voltage range between 23.5 kV and 26.0 kV for the TM_{11}-2π mode, and the output power changes from 1.58 kW to 3.15 kW in the

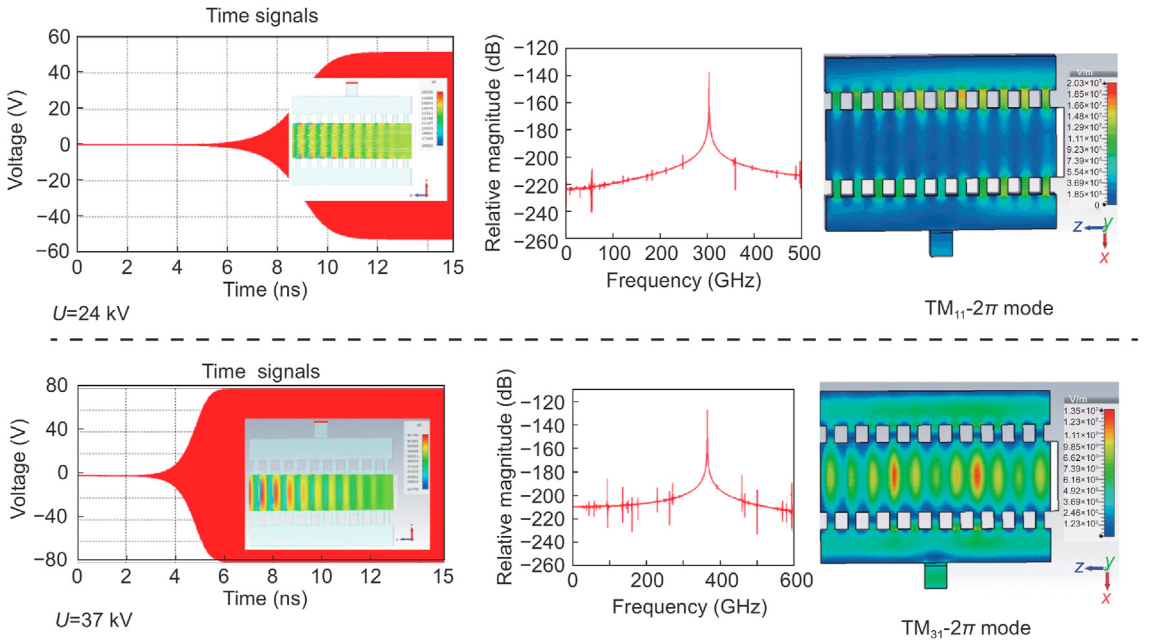

Fig. 8. Simulation results: Output voltage signals (inset: Trajectory of electrons), frequency spectra, and the electric field distributions at the operating voltages $U = 24$ kV (upside) and $U = 37$ kV (downside).

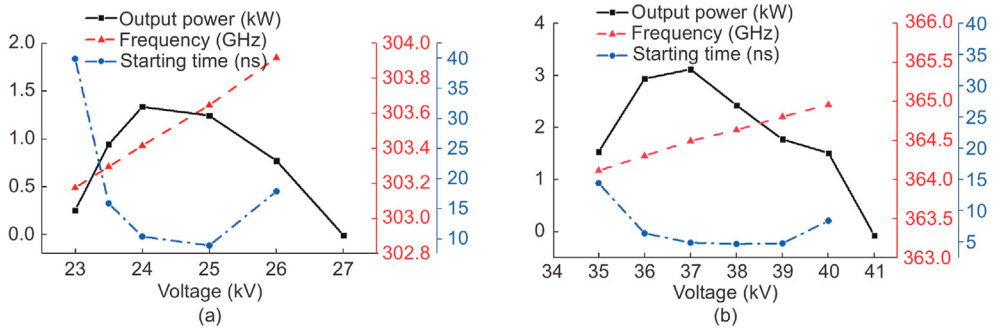

Fig. 9. Output power, frequency, and the oscillation starting time variations with the operating voltage: (a) TM_{11}-2π mode and (b) TM_{31}-2π mode.

voltage range between 35 kV and 40 kV for the TM_{31}-2π mode. The 3-dB tuning bandwidth is about 0.50 GHz and 0.84 GHz for the TM_{11}-2π and TM_{31}-2π modes with the maximum output power up to 1.34 kW and 3.18 kW, respectively. The simulation results show that the designed SEBEIO is stable for the TM_{11}-2π and TM_{31}-2π modes operation.

5. Conclusions

In this paper, the THz dual-mode EIO driven by PS-SEB was presented. Based on the analysis of the dispersion curve of the slow-wave structure and the electric field distribution in the cavity, the mode competition was studied. The PIC simulation predicts stable dual-mode operation, with the maximum output power of 1.34 kW, 3-dB bandwidth of ~0.50 GHz at 303.4 GHz when operating at the TM_{11}-2π mode, and the maximum output power of 3.18 kW, 3-dB bandwidth of ~0.84 GHz at 364.5 GHz when operating at the TM_{31}-2π mode, respectively. Our next step is to fabricate, assemble, and measure the designed dual-mode SEBEIO to verify the simulation results experimentally.

Funds

This research was supported by the National Natural Science Foundation of China under Grant No. 61771096; the Fundamental Research Funds for the Central Universities under Grant No. ZYGX2016J059; the National Basic Research Program of China under Grant No. 2013CB933603; in part by the UK Engineering and Physical Sciences Research Council (EPSRC) under Grant No. EP/S00968X/1.

Declaration of competing interest

The authors declare no conflicts of interest.

References

[1] P.H. Siegel, Terahertz technology, IEEE Trans. Microw. Theor. Tech. 50 (3) (Mar. 2002) 910–928.
[2] J.H. Booske, R.J. Dobbs, C.D. Joye, et al., Vacuum electronic high power terahertz sources, IEEE Trans. on Terahertz Science and Technology 1 (1) (Sept. 2011) 54–75.
[3] S.S. Dhillon, M.S. Vitiello, E.H. Linfield, et al., The 2017 terahertz science and technology roadmap, J. Phys. Appl. Phys. 50 (4) (Feb. 2017), 043001:1-49.
[4] J. Benford, J.A. Swegle, E. Schamiloglu, High Power Microwaves, third ed., CRC Press, Boca Raton, 2016.
[5] R.K. Parker, R.H. Abrams, B.G. Danly, et al., Vacuum electronics, IEEE Trans. Microw. Theor. Tech. 50 (3) (Mar. 2002) 835–845.
[6] M. Thumm, State-of-the-art of high-power gyro-devices and free electron masers, J. Infrared, Millim. Terahertz Waves 41 (1) (Jan. 2020) 1–140.
[7] J.H. Booske, Plasma physics and related challenges of millimeter-wave-to-terahertz and high power microwave generation, Phys. Plasmas 15 (5) (Feb. 2008), 055502:1-16.
[8] R.J. Barker, J.H. Booske, N.C. Luhmann Jr., G.S. Nusinovich, Modern Microwave and Millimeter-Wave Power Electronics, Wiley-IEEE Press, Hoboken, 2005.
[9] D. Berry, H. Deng, R. Dobbs, et al., Practical aspects of EIK technology, IEEE Trans. Electron. Dev. 61 (6) (Jun. 2014) 1830–1835.
[10] J. Christiansen, C. Schultheiss, Production of high current particle beams by low pressure spark discharges, Zeitschrift für Physik A Atoms and Nuclei 290 (1) (Mar. 1979) 35–41.
[11] H. Yin, A.D.R. Phelps, W. He, et al., A pseudospark cathode Cherenkov maser: Theory and experiment, Nucl. Instrum. Methods Phys. Res. Sect. A Accel. Spectrom. Detect. Assoc. Equip. 407 (1–3) (Apr. 1998) 175–180.
[12] H. Yin, G.R.M. Robb, W. He, A.D.R. Phelps, A.W. Cross, K. Ronald, Pseudospark-based electron beam and Cherenkov maser experiments, Phys. Plasmas 7 (12) (Aug. 2000) 5195–5205.
[13] H. Yin, A.W. Cross, A.D.R. Phelps, W. He, K. Ronald, Cherenkov interaction and post-acceleration experiments of high brightness electron beams from a pseudospark discharge, Nucl. Instrum. Methods Phys. Res. Sect. A Accel. Spectrom. Detect. Assoc. Equip. 528 (1–2) (Aug. 2004) 378–381.
[14] A.W. Cross, H. Yin, W. He, K. Ronald, A.D.R. Phelps, L.C. Pitchford, Generation and application of pseudospark-sourced electron beams, J. Phys. Appl. Phys. 40 (7) (Apr. 2007) 1953–1956.
[15] J. Pasour, E. Wright, K.T. Nguyen, et al., Demonstration of a multikilowatt, solenoidally focused sheet beam amplifier at 94 GHz, IEEE Trans. Electron. Dev. 61 (6) (Jun. 2014) 1630–1636.
[16] D. Gamzina, L.R. Barnett, B. Ravani, N.C. Luhmann, Mechanical design and manufacturing of W-band sheet beam klystron, IEEE Trans. Electron. Dev. 64 (6) (Jun. 2017) 2675–2682.
[17] J. Pasour, E. Wright, K. Nguyen, B. Levush, Compact, Multi-kW Sheet Beam Oscillator at 94 GHz," in Proc. Of the IEEE 41st Intl. Conf. on Plasma Sciences Held with IEEE Intl. Conf, on High-Power Particle Beams, Washington, 2014, p. 1.
[18] J.-X. Wang, X.-X. Li, L.-S. Rui, et al., Experimental Study of a 6 kW W-Band PCM Focused Sheet Beam EIO," in Proc. Of Intl. Vacuum Electronics Conf., Busan, 2019, pp. 1–2.
[19] G.-X. Shu, H. Yin, L. Zhang, et al., Demonstration of a planar W-Band, kW-level extended interaction oscillator based on a pseudospark-sourced sheet electron beam, IEEE Electron. Device Lett. 39 (3) (Mar. 2018) 432–435.
[20] G.-X. Shu, L. Zhang, H. Yin, et al., Experimental demonstration of a terahertz extended interaction oscillator driven by a pseudospark-sourced sheet electron beam, Appl. Phys. Lett. 112 (3) (Jan. 2018), 033504:1-21.
[21] K. Frank, E. Boggasch, J. Christiansen, et al., High-power pseudospark and BLT switches, IEEE Trans. Plasma Sci. 16 (2) (Apr. 1988) 317–323.
[22] W. Benker, J. Christiansen, K. Frank, et al., Generation of intense pulsed electron beams by the pseudospark discharge, IEEE Trans. Plasma Sci. 17 (5) (Oct. 1989) 754–757.
[23] P. Choi, H. Chuaqui, J. Lunney, R. Reichle, A.J. Davies, K. Mittag, Plasma formation in a pseudospark discharge, IEEE Trans. Plasma Sci. 17 (5) (Oct. 1989) 770–774.
[24] K. Frank, J. Christiansen, The fundamentals of the pseudospark and its applications, IEEE Trans. Plasma Sci. 17 (5) (Oct. 1989) 748–753.
[25] M.A. Gundersen, G. Schaefer, Physics and Applications of Pseudosparks, Plenum, New York, 1990.
[26] H. Yin, A.W. Cross, W. He, A.D.R. Phelps, K. Ronald, Pseudospark experiments: Cherenkov interaction and electron beam post-acceleration, IEEE Trans. Plasma Sci. 32 (1) (Feb. 2004) 233–239.
[27] H. Yin, A.W. Cross, W. He, et al., Millimeter wave generation from a pseudospark-sourced electron beam, Phys. Plasmas 16 (6) (Jun. 2009), 063105:1-6.
[28] W. He, L. Zhang, D. Bowes, et al., Generation of broadband terahertz radiation using a backward wave oscillator and pseudospark-sourced electron beam, Appl. Phys. Lett. 107 (13) (Sept. 2015), 133501:1-4.
[29] H.-B. Yin, L. Zhang, J. Xie, et al., Compact high-power millimetre wave sources driven by pseudospark-sourced electron beams, IET Microw., Antennas Propag. 13 (11) (Sept. 2019) 1794–1798.
[30] J. Xie, L. Zhang, H.-B. Yin, et al., Study of a 0.35 THz extended interaction oscillator driven by a pseudospark-sourced sheet electron beam, IEEE Trans. Electron. Dev. 67 (2) (Feb. 2020) 652–658.
[31] J. Zhang, T.-Z. Zhang, Y. Alfadhl, et al., Study on wideband THz backward wave oscillator driven by pseudospark-sourced sheet electron beam, IEEE Trans. Electron. Dev. 67 (8) (Aug. 2020) 3395–3402.
[32] Varun, U.N. Pal, PIC simulation to analyze peak electron current generation in a triggered pseudospark discharge-based plasma cathode electron source, IEEE Trans. Electron. Dev. 65 (4) (Apr. 2018) 1542–1549.
[33] J. Zhao, H. Yin, L. Zhang, et al., Advanced post-acceleration methodology for pseudospark-sourced electron beam, Phys. Plasmas 24 (2) (Feb. 2017), 023105:1-5.
[34] A.W. Varun, Cross, K. Ronald, U.N. Pal, PIC simulation of pseudospark discharge-based plasma cathode electron source for the generation of high current density and energetic electron beam, IEEE Trans. Electron. Dev. 67 (4) (Apr. 2020) 1793–1796.
[35] H. Yin, A.W. Cross, A.D.R. Phelps, D. Zhu, W. He, K. Ronald, Propagation and post-acceleration of a pseudospark-sourced electron beam, J. Appl. Phys. 91 (8) (Apr. 2002) 5419–5422.
[36] N. Kumar, R.P. Lamba, A.M. Hossain, U.N. Pal, A.D.R. Phelps, R. Prakash, A tapered multi-gap multi-aperture pseudospark-sourced electron gun based X-band slow wave oscillator, Appl. Phys. Lett. 111 (21) (Nov. 2017), 213502:1-4.
[37] N. Kumar, U.N. Pal, D.K. Pal, R. Prajesh, R. Prakash, Experimental investigation of a 1 kA/cm^2 sheet beam plasma cathode electron gun, Rev. Sci. Instrum. 86 (1) (Jan. 2015), 013503:1-5.
[38] N. Kumar, D.K. Pal, R.P. Lamba, U.N. Pal, R. Prakash, Analysis of geometrical design parameters for high-energy and high-current-density pseudospark-sourced electron beam emission, IEEE Trans. Electron. Dev. 64 (6) (Jun. 2017) 2688–2693.
[39] N. Kumar, A.S. Jadon, P. Shukla, U.N. Pal, R. Prakash, Analysis of experimental results on pseudospark discharge-based electron beams with simulation model, IEEE Trans. Plasma Sci. 45 (3) (Mar. 2017) 405–411.
[40] Y. Yin, W.-L. He, L. Zhang, H.-B. Yin, C.W. Robertson, A.W. Cross, Simulation and experiments of a W-band extended interaction oscillator based on a pseudospark-sourced electron beam, IEEE Trans. Electron. Dev. 63 (1) (Jan. 2016) 512–516.
[41] C. Xu, L. Meng, Y. Yin, et al., THz radiation from a high-order mode sheet beam extended interaction oscillator with staggered grating, AIP Adv. 9 (8) (Aug. 2019), 085314:1-6.
[42] Y. Yin, L.-J. Bi, B. Wang, et al., Preliminary circuit analysis of a W-band high-power extended interaction oscillator with distributed hollow electron beam, IEEE Trans. Electron. Dev. 66 (7) (Jul. 2019) 3190–3195.

[43] X. Zhang, R. Zhang, Y. Wang, Research on a high-order mode multibeam extended-interaction oscillator with coaxial structure, IEEE Trans. Plasma Sci. 48 (6) (Jun. 2020) 1902–1909.
[44] J.C. Stephens, G. Rosenzweig, M.A. Shapiro, et al., Design of a 94 GHz photonic bandgap based extended interaction klystron amplifier, in *Proc. of 18th Intl. Vacuum Electronics Conf., London* (2017) 1–2.
[45] Y. Yin, W. He, L. Zhang, H. Yin, A.W. Cross, Preliminary design and optimization of a G-band extended interaction oscillator based on a pseudospark-sourced electron beam, Phys. Plasmas 22 (7) (Jul. 2015), 073102:1-11.
[46] M.P. Kirley, J.H. Booske, Terahertz conductivity of copper surfaces, IEEE Trans. on Terahertz Science and Technology 5 (6) (Nov. 2015) 1012–1020.

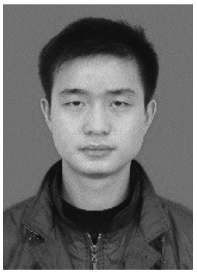

Jie Xie was born in Sichuan in 1989. He is currently pursuing the Ph.D. degree with the Vacuum Electronics National Laboratory, School of Electronic Science and Engineering, University of Electronic Science and Technology of China (UESTC), Chengdu. His current research interests include the millimeter waves & terahertz radiation sources based on vacuum electronics and the high-power microwave technique & its applications.

Xue-Song Yuan received the B.S. degree in physics from Anhui University, Hefei in 2002 and the Ph.D. degree in plasma physics from UESTC in 2008. He is currently an associate professor with the School of Electronic Science and Engineering, UESTC. His current research interests include millimeter waves and terahertz radiation generation, cold cathode particle beam generation, and radiation sources.

Liang Zhang received the B.S. degree in applied physics from University of Science and Technology of China, Hefei in 2004, the M.S. degree in applications of nuclear techniques from China Academy of Engineering Physics, Chengdu in 2007, and the Ph.D. degree in physics from University of Strathclyde, Glasgow in 2012. He is currently a research assistant with the Department of Physics, University of Strathclyde, Glasgow. His main research interests include the pulse power technology and gyrotron traveling-wave amplifiers (TWAs)/backward-wave oscillators.

Adrian W. Cross received the B.S. degree (with honors) in physics and Ph.D. degree from University of Strathclyde in 1989 and 1993, respectively. In 1993, he joined the Atoms, Beams, and Plasmas Group, University of Strathclyde, initially as a research fellow, and then became a lecturer in 2000, a senior lecturer in 2003, a reader in 2006, and a professor in 2014 with the Department of Physics. From 2002 to 2007, he was the Advanced Fellow of Engineering and Physical Sciences Research Council (EPSRC) and has been the Group Leader since 2014. He has been involved in various aspects of research on gyrotrons, cyclotron autoresonance masers, free-electron lasers, superradiant sources, gyrotron traveling-wave amplifiers, and plasma applications. More recently, he has primarily been concerned with research on microwave pulse compression, terahertz radiation sources, and pseudospark physics.

Hua-Bi Yin received the B.Eng. degree from Huazhong University of Science and Technology, Wuhan in 1983, the M.S. degree from China Academy of Engineering Physics in 1988, and the Ph.D. degree in physics from the Department of Physics, University of Strathclyde in 1998. She is currently a research fellow with the Department of Physics, University of Strathclyde. Her research interests include the area of the pulsed-power technology, pseudospark discharges, intense electron beam production, and microwave sources based on beam-wave instabilities.

Qing-Yun Chen was born in Jiangsu in 1991. She received the Ph.D. degree in plasma physics from the School of Electronic Science and Engineering, UESTC in 2020. Her current research interests include the millimeter waves & terahertz radiation sources based on vacuum electronics and the high-power microwave technique & its applications.

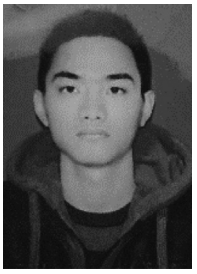

Tong-Bin Yang was born in Hunan in 1990. He is currently pursuing the Ph.D. degree with the Vacuum Electronics National Laboratory, School of Electronic Science and Engineering, UESTC. His current research interests include the millimeter waves & terahertz radiation sources based on vacuum electronics and the high-power microwave technique & its applications.

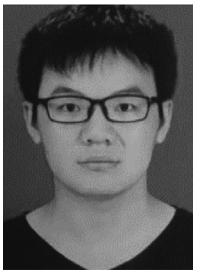

Xiao-Tao Xu was born in Hubei in 1994. He is currently pursuing the Ph.D. degree with the Vacuum Electronics National Laboratory, School of Electronic Science and Engineering, UESTC. His current research interests include the millimeter waves & terahertz radiation sources based on vacuum electronics and the high-power microwave technique & its applications.

Yang Yan received the B.S. and Ph.D. degrees from UESTC in 1986 and 1995, respectively. He is currently engaged in research with the Terahertz Researcher Center, UESTC, as a professor, where he is involved in the areas of gyrotrons, laser fusion, free-electron lasers, high-power microwaves, and fundamental plasma physics.

Lin Meng received the Ph.D. degree in physical electronics from UESTC in 1993. From 2001 to 2002, he was a Senior Visiting Fellow with the Department of Physics, Yale University, New Haven. Since 2001, he has been a professor with UESTC. His current research interests include plasma physics and the high-power microwave technique & its applications.